^{1}H NMR Analysis of Chain Unsaturations in Ethene/1-Octene Copolymers Prepared with Metallocene Catalysts at High Temperature

Vincenzo Busico,[†] Roberta Cipullo,[†] Nic. Friederichs,[‡] Harrie Linssen,[§] Annalaura Segre,[||] Valeria Van Axel Castelli,*[,†] and Geert van der Velden[§]

Dipartimento di Chimica, Università di Napoli "Federico II", Via Cintia, 80126 Naples, Italy, SABIC EuroPetrochemicals R&D, P.O. Box 319, 6160 AH Geleen, The Netherlands, DSM Resolve, P.O. Box 18, 6160 MD Geleen, The Netherlands, and Istituto di Metodologie Chimiche, CNR, M.B. 10, 00016 Monterotondo Stazione, Italy

Received March 24, 2005; Revised Manuscript Received May 4, 2005

ABSTRACT: In this paper, we report the full resonance assignments in the olefinic region of the 600 MHz ^{1}H NMR spectra of a typical ethene/1-octene copolymer (4.0 mol % of octene units) produced with a metallocene catalyst at high temperature, and of an ethene homopolymer prepared under similar conditions for comparison. The assignments were based on a thorough analysis of 1D (^{1}H, ^{1}H{^{1}H}, ^{13}C) spectra and of 2D ^{1}H−^{1}H (COSY, TOCSY) and ^{1}H−^{13}C (HSQC, DEPT-HSQC) maps. Thirteen different olefinic structures were identified, and their formation explained in terms of plausible mechanistic paths associated with the high polymerization temperature. The fraction of internal chain unsaturations traceable to allylic activation turned out to be comparable to that of terminal ones in both samples. Despite its complexity, the said spectral region is now amenable to deconvolution and full simulation in terms of known and recognizable patterns, and usable for fast (possibly on-line) measurements of chain unsaturation degree, as well as for catalyst "fingerprinting" studies.

Introduction

A most important advantage of single-center olefin polymerization catalysts, compared with the classical heterogeneous Ziegler−Natta ones, is their ability to afford copolymers with a narrow composition distribution. As a matter of fact, metallocene and half-metallocene (Constrained-Geometry) catalysts have found industrial application so far primarily in the copolymerizations of ethene with higher 1-alkenes (such as, e.g., 1-butene, 1-hexene, 1-octene), to give materials comprehensively referred to as Linear-Low-Density Poly(Ethylene) (LLDPE).[1]

Incorporating a 1-alkene comonomer into a polyethylene chain leads to a substantial decrease of the average polymerization degree, because chain transfer is faster (relative to propagation) after 1-alkene insertion. This translates into an inadequate molecular weight capability for numerous otherwise very attractive single-center catalysts, particularly in high-temperature processes.[2] A thorough chain end analysis of the polymers obtained is crucial in order to understand the nature and the relative importance of the various possible chain transfer pathways, preliminarily to catalyst tuning aimed at achieving a more favorable balance with chain propagation.

We have undertaken such a study, by means of 1D and 2D NMR spectroscopy, on ethene/1-octene copolymers, and also—for comparison—on ethene homopolymers prepared at high temperature (180−230 °C) in a solution batch process, using a number of C_2- and C_s-symmetric *ansa*-zirconocene[1,3] and constrained-geometry Ti catalysts[4] with borate activation. Although such temperatures exceed those typically encountered in gas-phase and slurry polymerizations, they are not uncommon for solution technologies.[2] Under the said conditions, we found that practically all chain terminations are unsaturated, and descend from a first event of β-H transfer to the metal or to the monomer. Despite a notable complexity, partly due to the contribution of several concurrent pathways of chain isomerization and allylic activation leading to the formation of internal unsaturations,[5] for all copolymers investigated we observed qualitatively similar olefinic "fingerprints", which could be fully assigned, and explained within a reasonably limited set of consolidated mechanistic assumptions. In this paper, we illustrate quantitative results for a representative ethene/1-octene copolymer with an octene content of 4.0 mol % (from here on denoted as sample **CP**), and for its reference ethene homopolymer (sample **HP**).

Experimental Section

Samples for solution NMR studies were prepared by dissolving 15 mg of polymer in 0.7 mL of tetrachloroethane-1,2-d_2 in a standard 5 mm NMR tube.

^{1}H, ^{1}H{^{1}H}, ^{13}C{^{1}H}, ^{1}H−^{1}H COSY, ^{1}H−^{1}H TOCSY, ^{1}H−^{13}C HSQC, and ^{1}H−^{13}C DEPT-HSQC experiments[6] were carried out at 343 K for sample **CP**, or 383 K for sample **HP**,[7] with a Bruker AQS-Avance 600 instrument, operating at 600.13 MHz (for ^{1}H), using a broadband inverse probe with *z*-gradient selection (for ^{1}H and 2D experiments), or a dual (^{13}C, ^{1}H) probe (for the ^{13}C experiment). Typical operating parameters were as follows.

^{1}H, ^{1}H{^{1}H}NMR: 8.4 μs (90° pulse) pulse width, 32K time domain data point, 8.4 kHz spectral width, 2 s acquisition time, 3 s relaxation delay, 512 transients. The ^{1}H homonuclear decoupled spectrum was performed by irradiating the allylic protons with a soft pulse, centered at 1.97 ppm (width, 80 Hz).

^{13}C{^{1}H} NMR: 7.2 μs (90° pulse) pulse width, 128K time domain data point, 36 kHz spectral width, 1.8 s acquisition time, 3.2 s relaxation delay, 10K transients, gated ^{1}H-decoupling with WALTZ16 composite pulse decoupling.[8]

2D gs-COSY NMR: 8.4 μs (90° pulse) pulse width, 7.2 kHz spectral width, 0.14 ms acquisition time, 1 s relaxation delay,

* Corresponding author. E-mail: valeria.vanaxel@imc.cnr.it.
[†] Università di Napoli "Federico II".
[‡] SABIC EuroPetrochemicals R&D.
[§] DSM Resolve.
[||] Istituto di Metodologie Chimiche, CNR.

10.1021/ma050620q CCC: $30.25
Published on Web 07/15/2005

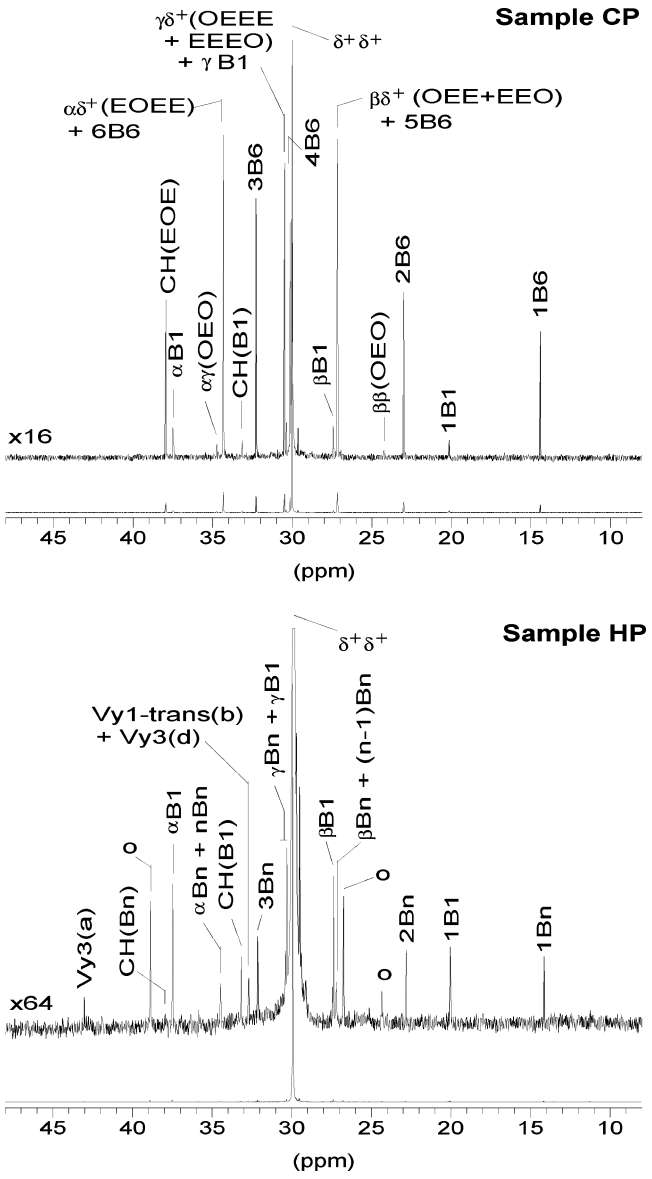

Figure 1. 150.9 MHz ^{13}C NMR spectrum of sample **CP** (top) and **HP** (bottom). The chemical shift scale is in ppm downfield of TMS. Peak attributions other than those in Table 1 are taken from the literature.[11] Peaks marked with ○ are due to impurities.

2K data points in F_2, 512 increments in F_1, 2K × 1K data matrix, 80 transients. Unshifted sinebell weighting functions were used for processing before Fourier transformation.

2D gs-TOCSY NMR: 8.4 μs (90° pulse) pulse width, 7.2 kHz spectral width, 0.14 s acquisition time, 1 s relaxation delay, 150 ms mixing time, 7 kHz spin-lock field with MLEV-17 composite pulse, 2K data points in F_2, 512 in F_1, 2K × 1K data matrix, 136 transients. These experiments were performed in phase-sensitive mode with TPPI phase cycle. Shifted squared sinusoidal weighting functions were used for processing before Fourier transformation.

2D gs-HSQC and 2D gs-DEPT-HSQC: 8.4 μs (90° pulse) pulse width, 7.2 kHz spectral width in the ^{1}H dimension, 27 kHz in the ^{13}C dimension, 0.14 s acquisition time, 1 s relaxation delay, 1K data points in F_2, 512 increments in F_1, 1K × 1K data matrix, ^{13}C GARP decoupling. A ^1J(C,H) = 145 Hz was considered, and 172 transients were collected in the HSQC experiment. ^{1}H−^{13}C correlation via double INEPT transfer (DEPT-HSQC)[6b] was performed in phase sensitive mode (echo−antiecho) with presaturation of the most intense signal (methylenes in the main chain). In this case ^1J(C,H) = 130 Hz was applied, and 172 transients were collected.

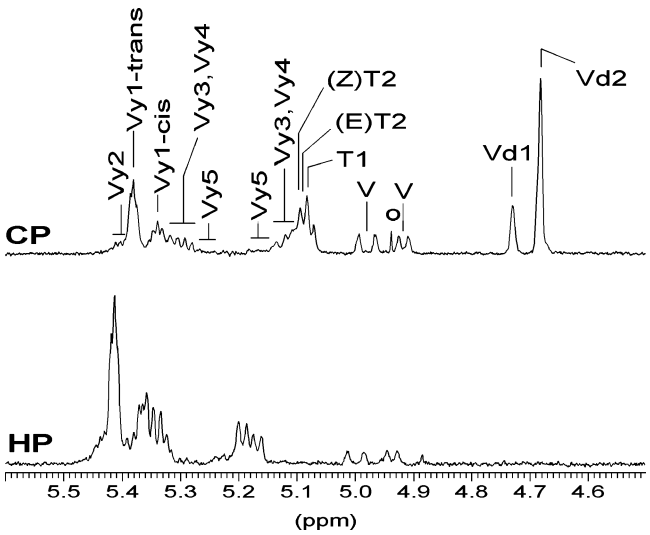

Figure 2. Olefinic region of the 600.13 MHz ^{1}H NMR spectrum of sample **CP** (top) and **HP** (bottom). The chemical shift scale is in ppm downfield of TMS. For peak attributions, refer to Table 1. The peak marked with ○ is due to a solvent impurity.

Exponential weighting functions in the case of the HSQC experiments, and shifted squared sinusoidal weighting functions in that of DEPT-HSQC, were used for processing before Fourier transformation.

Chemical shift values are referred to the signal of the solvent, set at 5.940 ppm in the ^{1}H spectrum, and at 74.30 ppm in the ^{13}C spectrum (downfield of TMS). The experimental error on the coupling constants J is ±0.5 Hz.

Deconvolutions and simulations of ^{1}H NMR spectra were carried out with the SHAPE-2004[9] and the Bruker NMR-SIM programs,[10] respectively.

Results and Discussion

(i) Resonance Assignment. The ^{13}C NMR spectra of the two samples, with the assignments taken from the literature,[11] are shown in Figure 1. An overnight accumulation (10K transients) resulted in a threshold for peak detectability of the order of 0.05% of the total integral. For sample **CP**, resonances indicative of consecutive octene units were not detected, which indicates a tendency of the comonomers to alternate ($r_E r_O < 1$). Methyl branches were observed at a concentration of 3 per 1000 C atoms of the main chain; ethyl, propyl, and butyl branches were below detectability, whereas longer branches could not be discriminated from the hexyl side groups of octene units. Sample **HP** showed a similar content of short branches (methyl, 2 per 1000 main chain C atoms; ethyl, propyl, and butyl, undetectable); in the absence of octene units, it was possible here to measure the cumulative fraction of longer branches, which turned out to be 0.7 per 1000 main chain C atoms.

The ^{1}H NMR spectra in the olefinic region (5.85−4.55 ppm downfield of TMS) are shown in Figure 2. A plethora of chain unsaturations gave rise to a large number of partly overlapped peaks in the spectra from both samples. A substantial simplification could be achieved by means of a ^{1}H{^{1}H} experiment, in which the allylic protons resonating in the 2.03−1.90 ppm range were selectively irradiated; for sample **CP** this is shown in Figure 3.

The spectrum of sample **CP** is—obviously—more complex, because it includes structures arising from last-inserted ethene units (in common with sample **HP**)

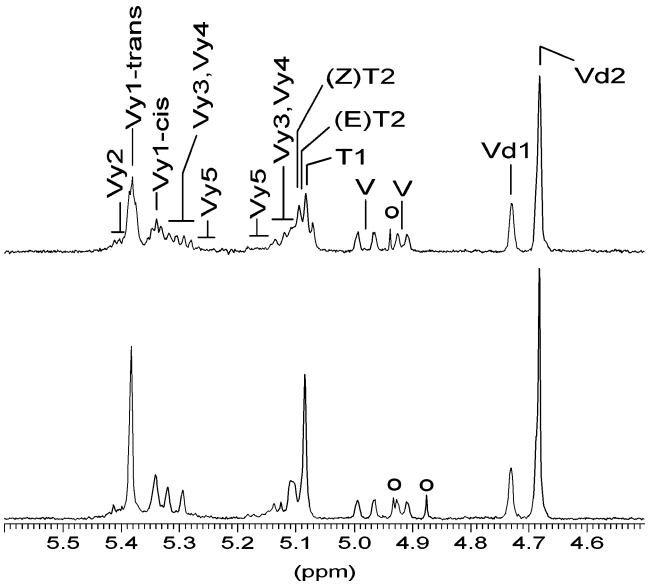

Figure 3. Comparison of the olefinic region in the 600.13 MHz ^{1}H (top) and ^{1}H{^{1}H} (bottom) NMR spectrum of sample **CP**. The chemical shift scale is in ppm downfield of TMS. Peaks marked with ○ are due to a solvent impurity. In the homodecoupled experiment, the allylic protons resonating in the 2.03−1.90 ppm range were selectively irradiated.

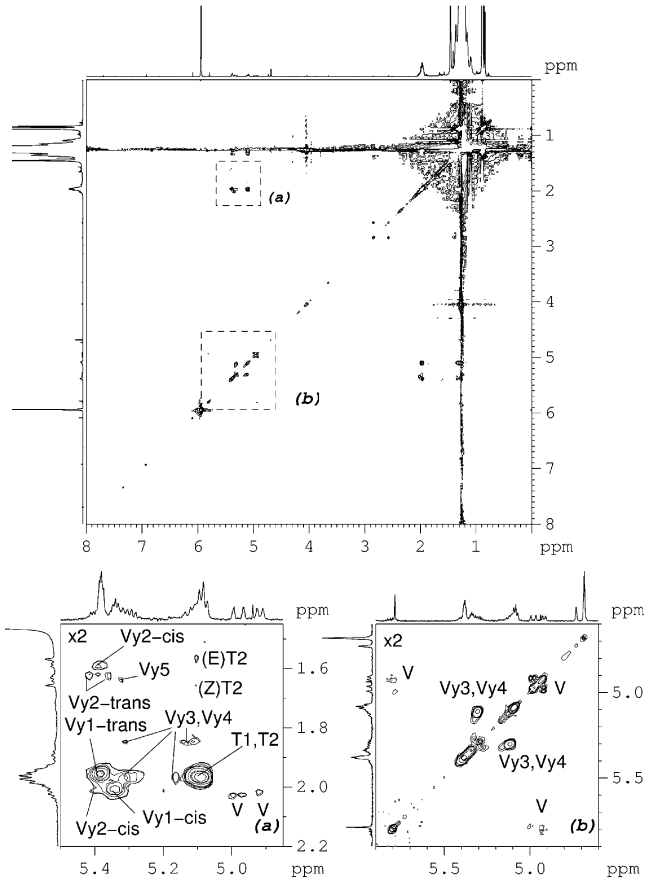

Figure 4. ^{1}H−^{1}H TOCSY map of sample **CP**, with selected enlargements.

and octene units as well; therefore, as far as resonance assignments are concerned, in the following we will refer primarily to **CP** sample.

A thorough analysis of the 1D spectra, of the ^{1}H−^{1}H COSY (Supporting Information) and TOCSY (Figure 4) maps, of the ^{1}H−^{13}C HSQC map (Supporting Information), and of the ^{1}H−^{13}C DEPT-HSQC map (Figure 5) led us to assign all unsaturated moieties with reasonable confidence. A summary of the identified structures, with their accessible ^{1}H and ^{13}C NMR data, is given in the first four columns of Table 1. The simulated individual patterns, and overall simulated spectra in comparison with the experimental ones (vide infra), are shown in Figures 6 and 7 (for the ^{1}H and the ^{1}H{^{1}H} experiment, respectively). In line with the previous literature,[12,13] distinctive ranges of ^{1}H chemical shift could be associated with the various structural types present, namely (from low to high field): vinylenes (RHC=CHR′), 5.5−5.1 ppm; trisubstituted olefins (RHC=CR′R″), 5.2−4.9 ppm; vinyls (CH_2=CHR), 5.0−4.8 ppm; vinylidenes (CH_2=CRR′), 4.8−4.6 ppm. In the following paragraphs, we discuss in more detail the spectral patterns observed for each range.

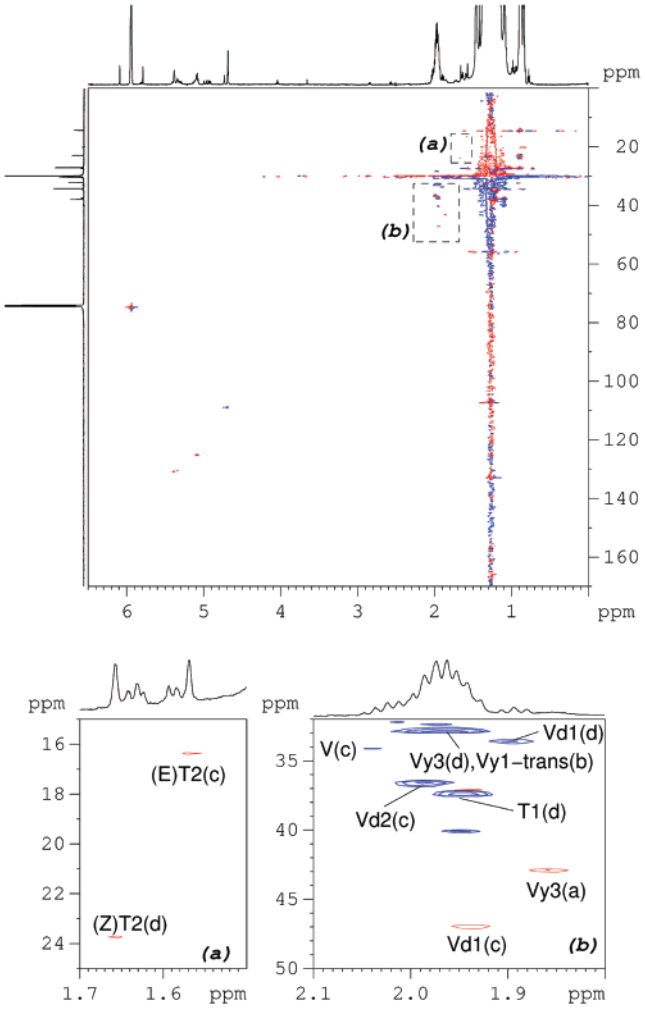

Figure 5. ^{1}H−^{13}C DEPT-HSQC map of sample **CP**, with selected enlargements (in red, positive cross-peaks due to CH and CH_3; in blue, negative cross-peaks due to CH_2).

Vinylenes. The two triplets at 5.38 ppm (J = 3.6 Hz) and 5.34 ppm (J = 4.7 Hz) are typical of *trans* and *cis* vinylene protons, respectively. The fact that the two protons in each couple have identical chemical shifts and do not reveal the typical vicinal couplings (~10 and ~14 Hz for *cis* and *trans* protons, respectively) indicates that the two alkyl substituents on the double bond are very similar, and points to structures **Vy1-*trans* and Vy1-*cis***. The observed multiplicity of **Vy1**-a is obviously due to the coupling with geminal methylene protons (**Vy1**-b); these resonate at 1.96 ppm in the case of **Vy1-**

Table 1. ^{1}H and ^{13}C NMR Data Relative to the Various Chain Unsaturations in the Investigated Polymer Samples

Structure	Notation	^{1}H NMR data (chemical shifts in ppm, multiplicities,[a] coupling constants (*J*) in Hz)	^{13}C NMR chemical shifts in ppm	Mole fraction[b] ×10^{3}		Location in the chain
				Sample **CP**	Sample **HP**	
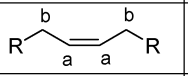	**Vy1-*cis***	a: 5.34; t ; *J* = 4.7 b: 2.01; m	a: 130.3 b: 27.4	0.27	0.44	Mostly Terminal
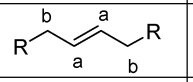	**Vy1-*trans***	a: 5.38; t ; *J* = 3.6 b: 1.96; m	a: 130.7 b: 32.7	0.49	1.52	Mostly Terminal
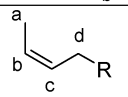	**Vy2-*cis***	a: 1.59; d; *J* = 6.7 b: 5.40; m c: 5.36; m d: 2.02; m		0.05	0.20	Terminal
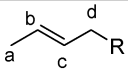	**Vy2-*trans***	a: 1.63; d; *J* ~ 7 b: 5.37; m c: 5.41; m d: 1.96; m		0.05	0.20	Terminal
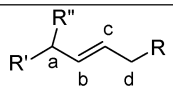	**Vy3**	a: 1.86; m b: 5.11; dd; *J* = 15.5, 7.7 c: 5.30; dt; *J* = 15.5, 7.2 d: 1.97; m	a: 42.8 b: 135.4 c: 130.1 d: 32.7	0.36	1.36	Internal
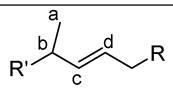	**Vy4**	a: 0.94; d; *J* = 6.7 b: 2.01; m c: 5.11; m d: 5.30; m		0.04	0.08	Internal
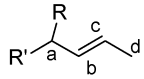	**Vy5**	a: 1.97; m b: 5.16; dd; *J* = 14.8, 6.5 c: 5.32; m d: 1.64; d; *J* ~ 7		0.09	0.12	Internal
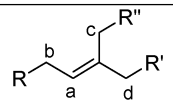	**T1**	a: 5.08 ; t ; *J* = 7.2 b: 1.97; m d: 1.94	a: 125.4 b: 28.0 d: 37.3	0.72	Not Detected	Internal
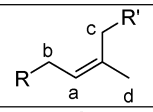	(*Z*)**T2**	a: 5.11; m b: 1.95; m d: 1.66; s	a: 126.7 d: 23.5	0.22[c]	Not Detected	Terminal
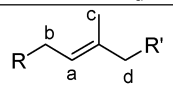	(*E*)**T2**	a: 5.09; m b: 1.97; m c: 1.57; s	a: 125.1 c: 16.2	0.13[c]	Not Detected	Terminal
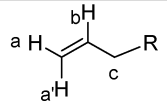	**V**	a: 4.917; d; *J* = 10.0 a': 4.979; d; *J* = 17.1 b: 5.81; ddt; *J* = 17.1, 10.0, 6.5 c: 2.03; m	c: 34.1	0.27	0.40	Terminal
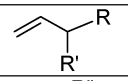	**V'**			Not Detected	Not Detected	
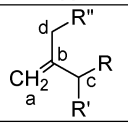	**Vd1**	a: 4.729; s c: 1.94 d: 1.89	c: 46.9 d: 33.6	0.18	Not Detected	Internal
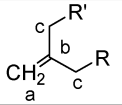	**Vd2**	a: 4.682; s c: 1.98	a: 108.7 c: 36.5	0.63	Not Detected	Terminal

[a] s, singlet; d, doublet; t, triplet; m, multiplet. [b] Uncertainty, ±5 × 10^{-5}. [c] Deriving from thermal isomerization of **Vd2** (via migration of the double bond).

trans, and at 2.01 ppm in that of **Vy1-*cis***, as shown by the ^{1}H−^{1}H correlation experiments (see, in particular, the TOCSY map). Consistent with the assignment, both triplets became singlets after selective irradiation of the allylic protons.

In the 5.41−5.36 ppm range, other multiplets are partially overlapped with the triplet of **Vy1-*trans***, which in the TOCSY map show cross-peaks with two doublets at 1.59 ppm (*J* = 6.7 Hz) and 1.63 ppm (*J* ~ 7 Hz), a region typical of resonances from methyls α to a double bond.[12,13] Therefore, we assigned the said signals to **Vy2** structures; in particular, based on the literature,[12a] the methyl at 1.63 ppm was attributed to **Vy2-*trans*** and that at 1.59 ppm to **Vy2-*cis***. Selective irradiation of the allylic methylenes led to a partial simplification of the multiplets, as expected.

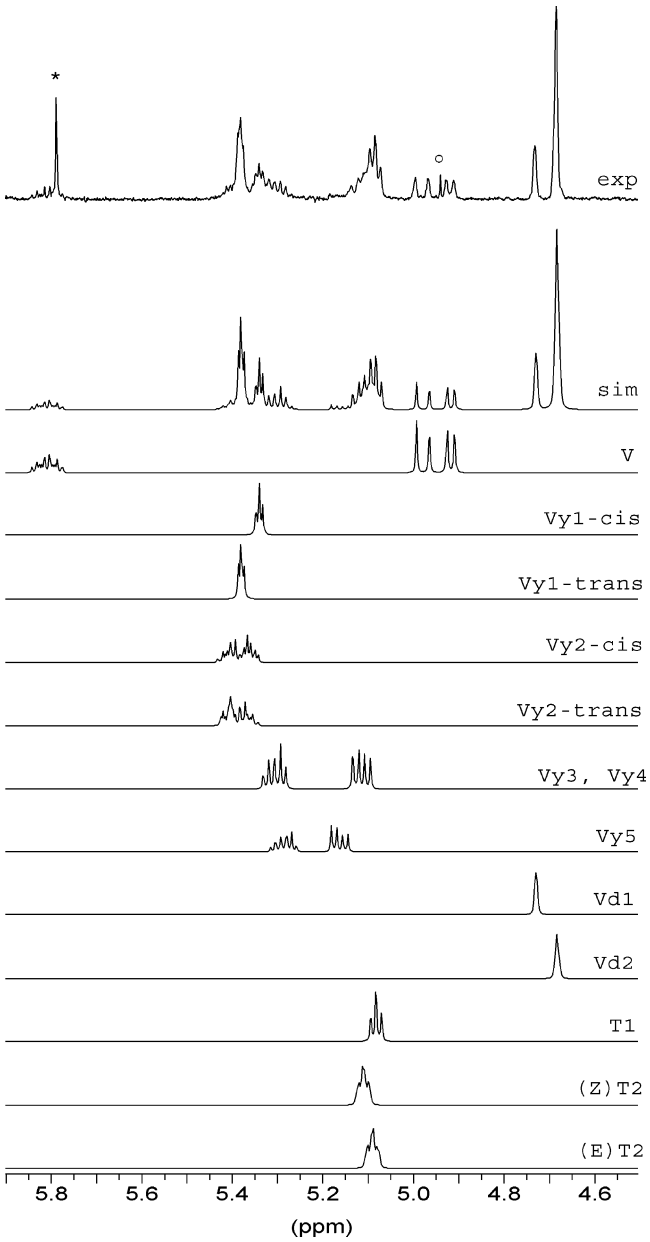

Figure 6. Olefinic region of the 600.13 MHz ^{1}H NMR spectrum of sample **CP**. First trace from top: experimental spectrum (∗, solvent satellite; ○, solvent impurity). Second trace from top: fully simulated spectrum. Lower traces: simulated patterns of the individual structures assigned.

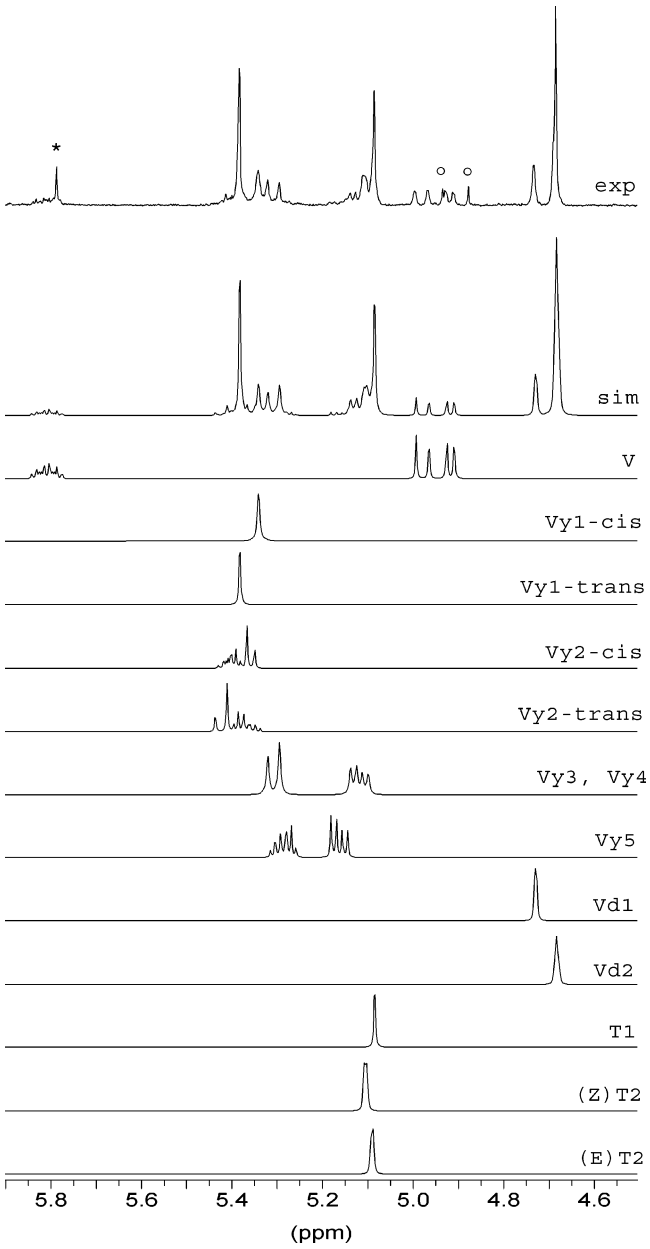

Figure 7. Olefinic region of the 600.13 MHz ^{1}H{^{1}H} NMR spectrum of sample **CP**. First trace from top: experimental spectrum (∗, solvent satellite; ○, solvent impurity). Second trace from top: fully simulated spectrum. Lower traces: simulated patterns of the individual structures assigned.

A third pattern consists of a doublet of triplets centered at 5.30 ppm (J = 15.5, 6.7 Hz), shown by COSY and TOCSY to correlate with a multiplet at 5.11 ppm. The former signal also correlates with the resonances of the allylic methylenes at 1.97 ppm; the latter resonance is, instead, correlated with a resonance at 1.86 ppm that by ^{1}H−^{13}C DEPT-HSQC was proven to be a methine group, with a ^{13}C chemical shift of 42.8 ppm (see Figure 5, expansion b). Perusal of the literature[12g,h] led us to assign this pattern to structure **Vy3**, in which the allylic methine carries two alkyl residues larger than methyl; the observed coupling constant for the two olefinic protons **Vy3**-b and **Vy3**-c (J = 15.5 Hz) indicates that these are in *trans* configuration. We ascribe the unusually high-field value of ^{1}H chemical shift of **Vy3**-a to a rigid conformation imposed by the two sterically demanding alkyl substituents, forcing the proton in question out of the deshielding cone of the double bond. The assignment is consistent with a calculated ^{13}C chemical shift value for **Vy3**-a of 42.4 ppm (according to the CSPEC method[14]), and also with the results of the ^{1}H{^{1}H} experiment; in fact, selective irradiation of the allylic protons in the 2.03−1.90 ppm range (including the **Vy3**-d protons) changed the double triplet of **Vy3**-c at 5.30 ppm into a doublet (J = 15.5 Hz), due to residual coupling with **Vy3**-b. The multiplet at 5.11 ppm, on the other hand, was unaffected, because proton **Vy3**-a at 1.86 ppm was not irradiated.

In the aliphatic region of the ^{1}H spectrum, a very weak doublet centered at 0.94 ppm was detected, indicative of a methyl β to a double bond[12,13] and coupled to one proton. The COSY map clarified that the latter is an allylic methine proton with δ = 2.01 ppm. We assigned the said signals to structure **Vy4** (whose olefinic protons are magnetically undistinguishable from those of **Vy3**).

One more pattern, composed of two proton resonances at 5.32 and 5.16 ppm, barely emerged from the noise. In the TOCSY map, the signal at 5.32 ppm is correlated to a doublet at 1.64 ppm ($J \sim 7$ Hz), indicating a methyl α to a double bond. In view of the similarity with **Vy3** and **Vy4**, we tentatively assigned these signals to structure **Vy5**.

Trisubstituted Olefins. The triplet ($J = 7.2$ Hz) centered at 5.08 ppm, partly overlapped with the signal of **Vy3**-b, and strongly correlated in the TOCSY map with the multiplet at 1.97 ppm, was assigned to structure **T1**. In line with the assignment, it reduced to a singlet in the $^1H\{^1H\}$ experiment.

Additional weaker signals in this range were also visible. In particular, a multiplet centered at 5.11 ppm shows a weak correlation in the TOCSY map with a singlet at 1.66 ppm (diagnostic for a methyl α to a double bond, as noted before); this, in turn, in the $^1H-^{13}C$ HSQC map (see Supporting Information) correlates with a ^{13}C resonance at 23.5 ppm, which is a typical value for an allylic methyl in *cis* configuration with respect to an olefinic proton.[12b] All this, along with the fact that the quoted multiplet at 5.11 ppm reduced to a singlet in the homodecoupled experiment, points to structure ***(Z)*T2**. A second multiplet centered at 5.09 ppm weakly correlates with a singlet at 1.57 ppm (another allylic methyl), correlating in turn with a ^{13}C resonance at 16.2 ppm, typical of allylic methyls in *E* configuration;[12b] the pattern was then assigned to structure ***(E)*T2**. Importantly, as we shall see in a following paragraph, structures **T2** do *not* originate from the polymerization, but from the thermal isomerization of a vinylidene.

Vinyls. The doublets at 4.979 ppm ($J = 17.1$ Hz) and 4.917 ppm ($J = 10.0$ Hz) could be easily assigned to the two geminal protons of structure **V**; in particular, by comparison of the *J* values with literature ones, the signal at higher field was attributed to proton **V**-a, the other to proton **V**-a′. The assignment was confirmed by the COSY and TOCSY maps, showing correlation spots between the quoted signals and a multiplet at 5.81 ppm due to proton **V**-b. In the $^1H\{^1H\}$ spectrum, the latter was decoupled only in part from the neighboring allylic methylene protons **V**-c, which resonates at 2.03 ppm, and therefore were not completely saturated by the soft pulse centered at 1.97 ppm.

Vinylidenes. The two signals at 4.729 and 4.682 ppm are *not* correlated in the $^1H-^1H$ maps (Figure 4 and Supporting Information). We assigned them to the geminal protons of two different vinylidene structures. To increase the resolution of the signals and thus reveal the allylic coupling (usually $J = 0-2$ Hz), a strong Gaussian apodization function was applied to the FID, with the result shown in Figure 8. For the signal at lower field, the quartet pattern ($J = 1.6$ Hz) points to structure **Vd1**. The signal at higher field, in turn, appears as the superposition of two close-by triplets, and is compatible with structure **Vd2**, in which both alkyl substituents of the double bond have an α-methylene, but differ somehow at more distant locations. As expected, the vinylidene signals remained unchanged in the $^1H\{^1H\}$ experiment.

During the spectral acquisition, **Vd2** showed a tendency to slowly isomerize[15] to **T2** (***Z*** and ***E***), as indicated by the fact that the signal at 4.682 ppm decreased and the signals at 5.11 and 5.09 ppm correspondingly increased with time.[16]

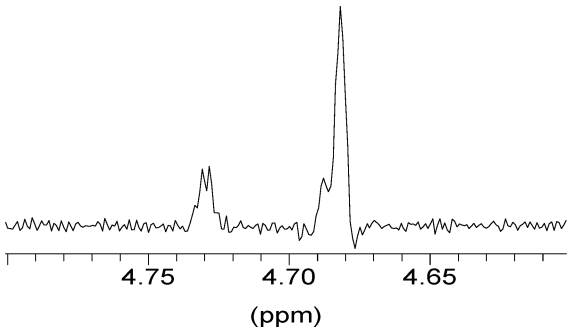

Figure 8. Vinylidene range of the ^1H NMR spectrum of sample **CP**, as obtained by FID processing with a strong Gaussian apodization function (see text).

(ii) Quantitative Evaluation of the Spectra. In columns 5 and 6 of Table 1, we report the mole fraction of each unsaturated structure for sample **CP** and **HP**, respectively, determined by deconvolution of the ^1H spectra. In the calculations, the normalized integrals of the olefinic protons were scaled to the average proton content of the monomeric units (4.48 for sample **CP**, 4.00 for sample **HP**; long chain branches not considered). Using these data, the olefinic region of the proton spectrum was fully simulated by summing up the individual simulated patterns of each assigned structure with the appropriate normalized integrals. The match with the experimental spectrum is very nice, as is shown for sample **CP** in Figures 6 (^1H experiment) and 7 ($^1H-\{^1H\}$ experiment).

(iii) Mechanistic Considerations. In Schemes 1 and 2, we propose plausible mechanistic paths leading to the formation of all observed unsaturations, starting from a growing chain with a last-inserted ethene or octene unit, respectively. Despite the apparent complexity, the chemistry involved is fairly straightforward, with an initial event of β-H transfer being followed in alternative by the following:

(i) macroolefin displacement (represented as dissociative but possibly monomer-assisted[3b,17]), which leads to a terminal unsaturation;

(ii) "allylic activation" of the chain,[5] i.e., attack of the hydride on M to the allylic methylene of the coordinated olefin, with formation and release of dihydrogen (H_2 evolution was indeed observed during the polymerizations), and of a coordinated allyl, which then undergoes monomer insertion;

(iii) in the specific case of a coordinated macrovinyl (**V**), rotation of the double bond and reinsertion into the M−H bond, which forms an α-methyl-branched polymeryl. This can then undergo monomer (in particular, ethene) insertion, or β-H elimination again. Sequences of β-H elimination, double bond rotation and reinsertion steps can lead to a migration of the double bond, and explain the observed formation of vinylene unsaturations and of long(er) branches. This route, extensively documented for late transition metal catalysts and commonly referred to as "chain walking",[18] is less important but not unprecedented for Group 4 metal catalysts,[19,20] and in the cases investigated here was probably favored by the high polymerization temperature.

In agreement with experiment (Table 1), Schemes 1 and 2 predict that structures **Vd1**, **Vd2**, **T1**, and **T2** are peculiar to copolymers, whereas all others are in common with ethene homopolymers. It may be worth noting that, although the hypothesis of occasional regioirregu-

Scheme 1. Possible Paths Leading to Chain Unsaturation for a Polymeryl with a Last-Inserted Ethene Unit

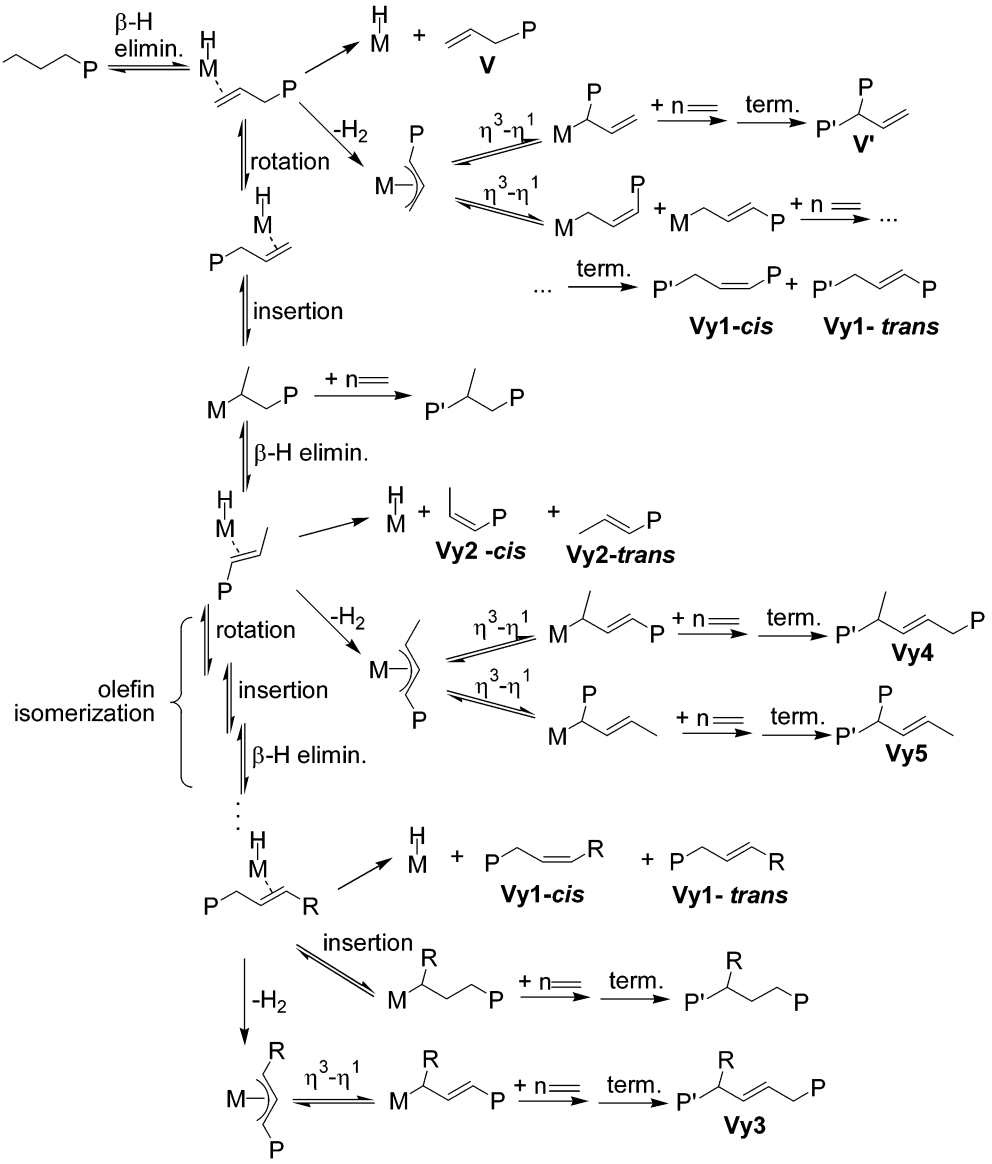

Scheme 2. Possible Paths Leading to Chain Unsaturation for a Polymeryl with a Last-Inserted Octene Unit

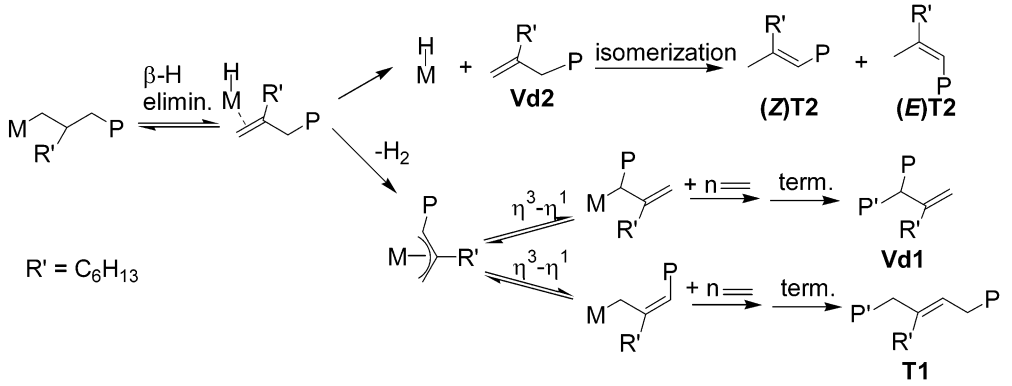

lar 2,1 insertions of 1-octene cannot be ruled out based on our experimental data, there is no need to invoke it to justify any of the observed chain unsaturations.

A classification of the olefinic structures as terminal (chain ends) or internal, which is obviously a prerequisite for the NMR-based calculation of number-average polymerization degree (P_n), can also be operated according to the schemes, and is reported in the last column of Table 1. Such a classification is trivial with just one exception: in fact, if structures **V**, **Vy2**, and **Vd2**+**T2** are necessarily chain ends, and **Vy3**, **Vy4**, **Vy5**, and **Vd1** internal unsaturations, **Vy1** can be either (with reference to Scheme 1, internal if derived from allylic activation of coordinated vinyl **V**; terminal if formed via

Table 2. Values of the Number Average Polymerization Degree (P_n) and Molecular Mass (M_n) as Calculated from the ^{1}H NMR Data (See Text), and Determined by Gel Permeation Chromatography for Comparison

	sample **CP**		sample **HP**	
	P_n	M_n, kDa	P_n	M_n, kDa
calculated by ^{1}H NMR (**Vy1** assumed as terminal)	4.7×10^2	15	3.6×10^2	10
calculated by ^{1}H NMR (**Vy1** assumed as internal)	7.4×10^2	23	1.2×10^3	35
determined by GPC	3.2×10^2	10	3.6×10^2	10

chain walking after a methyl branch formation). The above introduces an uncertainty in the NMR evaluation of P_n; however, assuming that **Vy1** is terminal leads to a reasonably good agreement between the calculated value and that determined by GPC, whereas overestimation of P_n results from the hypothesis that **Vy1** is internal (Table 2).

It is interesting to note that, of the five detected vinylene structures, **Vy1** and **Vy2** can occur in *trans* and *cis* configuration, whereas for **Vy3**, **Vy4**, and **Vy5** exclusively the *trans* isomer was observed. This is probably due to the fact that in the last three cases, according to our assignment (which then receives an indirect confirmation), one of the two alkyl substituents of the double bond is α-branched, which should enforce the thermodynamic preference for the *trans* over the *cis* configuration.

Altogether, structures **Vy3**, **Vy4**, **Vy5**, and **Vd1** provide a strong indication that olefin insertion at M-allyl species is viable; this is in line with the results of recent theoretical studies.[21] In Schemes 1 and 2, we assumed a step of η^3-to-η^1 allyl isomerization, known to favor the formation of the most substituted double bond and, correspondingly, of the least sterically encumbered M−(η^1-allyl), followed by a standard Cossee-type insertion into the M−C σ bond;[3b] this provides an immediate and simple explanation for the observed excess of **Vy5** over **Vy4**, and of **T1** over **Vd1**, as well as for the undetectability of **V′** (Table 1). On the other hand, direct olefin insertion into a M−(η^3-allyl) bond, as hypothesized in the aforementioned theoretical studies,[21] cannot be ruled out on the basis of our data, and might well be sterically governed in a similar manner. The large fraction of chain unsaturations traceable to this chemistry in the two investigated samples is due to the high polymerization temperature, making processes with higher activation energies more competitive.

Concerning the relative importance of the various possible pathways of chain transfer, from Table 1 it is easy to realize that roughly 50% of all terminal unsaturations in sample **CP** can be traced to β-H transfer from last-inserted octene units, although these amount to 4.0 mol % only; therefore, on average, the ratio $\langle P_t \rangle / \langle P_p \rangle$ between the (average, cumulative) conditional probabilities of chain transfer and propagation, under the specific conditions used for sample preparation, was ca. 20-fold larger after 1-octene than after ethene insertion.

Methyl branches, in turn, despite a low relative abundance, appear to be important generators of internal unsaturations, as being particularly prone to undergo β-H transfer followed by allylic activation (Scheme 1, bottom part).

Conclusions

In this paper, we have reported the full assignments of the resonances in the olefinic region of the ^{1}H NMR spectra of an ethene/1-octene copolymer produced with a metallocene catalyst at high temperature, and also—for comparison—of a similarly prepared ethene homopolymer. Thirteen different terminal and internal chain unsaturations (eight of which are observed in the reference homopolymer) were identified, and their formation explained in terms of a limited set of plausible mechanistic paths, originating from a first event of β-H transfer, possibly followed by allylic chain activation.

These results are useful in at least two respects. First, they make the said spectral region amenable to deconvolution and full simulation in terms of known and recognizable patterns, and usable for quantitative measurements of number-average molecular mass and unsaturation degree. Considering that the sensitivity of ^{1}H NMR is very high, and that data acquisition is correspondingly very fast, this achievement can be particularly relevant and advantageous in view of repetitive applications for quality control and high-throughput screening.

Second, we anticipate that although—as already noted in the Introduction—all ethene/1-octene copolymers examined in this study contain basically the same unsaturations, we have found out that the absolute and relative amounts of the various individual structures are dependent not only on the polymerization conditions (which is fairly obvious), but also on the specific catalyst used. This suggests that the olefinic pattern of a given copolymer sample can be used diagnostically as a catalyst "fingerprint". This concept will be elaborated in a separate paper.

Acknowledgment. We acknowledge Dr. Martin Roest, Mr. Jo Beulen, and Mrs. Gerda Kolfschoten for assistance in the NMR measurements that originated the present study.

Supporting Information Available: Figures showing ^{1}H NMR spectra of samples **CP** and **HP**, ^{1}H−^{1}H COSY map of sample **CP**, and ^{1}H−^{13}C HSQC map of sample **CP**. This material is available free of charge via the Internet at http://pubs.acs.org.

References and Notes

(1) General references: (a) Brintzinger, H. H.; Fischer, D.; Muelhaupt, R.; Rieger, B.; Waymouth, R. M. *Angew. Chem., Int. Ed. Engl.* **1995**, *34*, 1143−1170. (b) *Metallocene-Based Polyolefins: Preparation Properties and Technology*; Schiers, J., Kaminsky, W., Eds.; Wiley: Chichester, England, 2000.
(2) See, e.g.: (a) WO 97/22635 (Exxon Chemical Co.). (b) WO 93/08221 (Dow Chemical Co.). (c) DE 3150270 (Erdolchemie). (d) Yano, A.; Sone, M.; Yamada, S.; Hasegawa, S.; Sato, M.; Akimoto, A. *J. Mol. Catal., A* **2000**, *156*, 133−141. (e) Yano, A.; Sone, M.; Hasegawa, S.; Sato, M.; Akimoto, A. *Macromol. Chem. Phys.* **1999**, *200*, 933−941.
(3) For recent reviews, see: (a) Alt, H. G.; Koeppl, A. *Chem. Rev.* **2000**, *100*, 1205−1222. (b) Resconi, L.; Cavallo, L.; Fait, A.; Piemontesi, F. *Chem. Rev.* **2000**, *100*, 1253−1346.
(4) Review: McKnight, A. L.; Waymouth, R. M. *Chem. Rev.* **1998**, *98*, 2587−2598.
(5) Reference 3b, pp 1277−1278 and references therein.
(6) Generel references: (a) Braun, S.; Kalinowski, H.-O.; Berger, S. *150 and More Basic NMR Experiments*, 2nd ed.; Wiley:

Weinheim, Germany, 1998. (b) Willker, W.; Leibfritz, D.; Kerssebaum, R.; Bermel, W. *Magn. Reson. Chem.* **1993**, *31*, 287−292.

(7) The 40 K difference in acquisition temperature between the spectra of the two samples (made necessary by the high crystallinity of sample **HP**) resulted, of course, in slight differences of chemical shift values for corresponding peaks. For the ^{1}H spectra, in particular, we checked that with the used chemical shift scale calibration the said differences are within 10−30 Hz, which is not enough to result into appreciable changes in the spectral patterns of interest.

(8) Quantitative measurements on the ^{13}C NMR spectra were based on main chain C's, known to have practically identical NOE. Therefore, to maximize the *S*/*N* ratio, full NOE (rather than inverse gated) conditions were adopted.

(9) SHAPE-2004. Vacatello, M. University of Naples "Federico II". This software package has been developed specifically for the simulation of 1D NMR spectra of polymers. For inquiries: vacatello@chemistry.unina.it.

(10) http://www.bruker-biospin.de/NMR/nmrsoftw/prodinfo/nmr_suit/nmr-sim/.

(11) (a) Barrera Galland, G.; de Souza, R. F.; Santos Mauler, R.; Nunes, F. F. *Macromolecules* **1999**, *32*, 1620−1625. (b) Liu, W.; Rinaldi, L.; McIntosh, L. H.; Quirk, R. P. *Macromolecules* **2001**, *34*, 4757−4767.

(12) (a) Stehling, F. C.; Bartz, K. W. *Anal. Chem.* **1966**, *38*, 1467−1479. (b) Couperus, P. A.; Clague, A. D. H.; van Dongen, J. P. C. M. *Org. Magn. Reson.* **1976**, *8*, 426−431. (c) Babu, G. N.; Newmark, R. A.; Chien, J. C. W. *Macromolecules* **1994**, *27*, 3383−3388. (d) Rossi, A.; Zhang, J.; Odian, G. *Macromolucules* **1996**, *29*, 2331−2338. (e) Dang, V. A.; Yu, L.-C.; Balboni, D.; Dall'Occo, T.; Resconi, L.; Mercandelli, P.; Moret, M.; Sironi, A. *Organometallics* **1999**, *18*, 3781−3791. (f) Hasegawa, S. *J. Polym. Sci., A* **2000**, *38*, 4641−4648. (g) Belelie, J. L.; Chong, J. M. *J. Org. Chem.* **2001**, *66*, 5552−5555. (h) Harrington-Frost, N.; Leuser, H.; Calaza, M. I.; Kneisel, F. F.; Knochel, P. *Org. Lett.* **2003**, *5*, 2111−2114.

(13) Silverstein, R. M.; Bassler, G. C.; Morrill, T. C. *Spectrometric Identification of Organic Compounds*, 5th ed.; Wiley: New York, 1991; pp 215, 237−238.

(14) Cheng, H. N.; Bennett, M. A. *Anal. Chim. Acta* **1991**, *242*, 43−56.

(15) See, e.g.: Rieger, B.; Reinmuth, A.; Roell, W.; Brintzinger, H. H. *J. Mol. Catal.* **1993**, *82*, 67−73.

(16) The presence of minor amounts of tetrasubstituted double bonds (in particular deriving from the thermal isomerization of **Vd1**) cannot be ruled out. However, their undetectability in the ^{13}C and HSQC NMR spectra, and the substantial agreement between experimental and calculated integrals of the allylic protons in the ^{1}H NMR spectra indicate that such structures can be neglected.

(17) Fan, W.; Waymouth, R. M. *Macromolecules* **2001**, *34*, 8619−8625.

(18) For a recent review, see: Ittel, D. S.; Johnson, L. K.; Brookhart, M. *Chem. Rev.* **2000**, *100*, 1169−1204.

(19) (a) Busico, V.; Cipullo, R. *J. Am. Chem. Soc.* **1994**, *116*, 9329−9330. (b) Leclerc, M.; Brintzinger, H. H. *J. Am. Chem. Soc.* **1995**, *117*, 1651−1652. (c) Busico, V.; Caporaso, L.; Landriani, L.; Angelini, G.; Margonelli, A.; Segre A. L. *J. Am. Chem. Soc.* **1996**, *118*, 2105−2106. (d) Leclerc, M. K.; Brintzinger, H. H. *J. Am. Chem. Soc.* **1996**, *118*, 9024−9032. (e) Busico, V.; Cipullo, R.; Caporaso, L.; Angelini, G.; Segre, A. L. *J. Mol. Catal., Part A (Chem.)* **1998**, *128*, 53−64. (f) Yoder, J. C.; Bercaw, J. E. *J. Am. Chem. Soc.* **2002**, *124*, 2548−2555. (g) Sillars, D. R.; Landis, C. R. *J. Am. Chem. Soc.* **2003**, *125*, 9894−9895.

(20) (a) Harney, M. B.; Keaton, R. J.; Sita, L. R. *J. Am. Chem. Soc.* **2004**, *126*, 4536−4537. (b) Wang, W.-J.; Yan, D.; Zu, S.; Hamielec, A. E. *Macromolecules* **1998**, *31*, 8677−8683.

(21) (a) Margl, P. M.; Woo, T. K.; Ziegler, T. *Organometallics* **1998**, *17*, 4997−5002. (b) Lieber, S.; Prosenc, M.-H.; Brintzinger, H. H. *Organometallics* **2000**, *19*, 377−387. (c) Moscardi, G.; Resconi, L.; Cavallo, L. *Organometallics* **2001**, *20*, 1918−1931.

MA050620Q